Observations of the structure and evolution of surface and flight-level wind asymmetries in Hurricane Rita (2005)

Robert Rogers[1] and Eric Uhlhorn[1]

[1] Knowledge of the magnitude and distribution of surface winds, including the structure of azimuthal asymmetries in the wind field, are important factors for tropical cyclone forecasting. With its ability to remotely measure surface wind speeds, the stepped frequency microwave radiometer (SFMR) has assumed a prominent role for the operational tropical cyclone forecasting community. An example of this instrument's utility is presented here, where concurrent measurements of aircraft flight-level and SFMR surface winds are used to document the wind field evolution over three days in Hurricane Rita (2005). The amplitude and azimuthal location (phase) of the wavenumber-1 asymmetry in the storm-relative winds varied at both levels over time. The peak was found to the right of storm track at both levels on the first day. By the third day, the peak in flight-level storm-relative winds remained to the right of storm track, but it shifted to left of storm track at the surface, resulting in a 60-degree shift between the surface and flight-level and azimuthal variations in the ratio of surface to flight-level winds. The asymmetric differences between the surface and flight-level maximum wind radii also varied, indicating a vortex whose tilt was increasing. **Citation:** Rogers, R., and E. Uhlhorn (2008), Observations of the structure and evolution of surface and flight-level wind asymmetries in Hurricane Rita (2005), *Geophys. Res. Lett.*, 35, L22811, doi:10.1029/2008GL034774.

1. Introduction

[2] Accurately predicting the magnitude and distribution of surface winds in landfalling tropical cyclones (TC) is a top priority for the forecast community. A key component in improving these predictions is the collection of enhanced observations to better understand the factors that determine TC intensity and surface wind field structure. Research has focused on the role of storm motion and the associated asymmetries in frictional convergence in generating these asymmetries [*Kepert*, 2006a, 2006b; *Kepert and Wang*, 2001; *Kepert*, 2001; *Shapiro*, 1983]. These and earlier studies have found that peak storm-relative surface winds are generally found downwind of the maximum above the boundary layer, and the surface to flight-level wind ratio is maximized to the left (right) side of the storm track in the northern (southern) hemisphere.

[3] While these and other observational studies [*Schneider and Barnes*, 2005; *Reasor et al.*, 2000; *Marks and Houze*, 1987; *Powell*, 1987] have documented TC asymmetric wind field structure, the employed observational platforms (e.g., airborne Doppler radar, flight-level winds, dropsondes) each have their drawbacks for inferring surface winds. Airborne Doppler radar typically cannot sample the wind field below ~500 m [*Marks and Houze*, 1987] and it is not available on the Air Force reconnaissance aircraft. Flight-level winds are extrapolated to the surface using an empirical model [*Franklin et al.*, 2003] which may involve considerable uncertainty. Dropsondes provide direct surface measurements, but they are point measurements, so their temporal and spatial coverages are limited.

[4] The stepped frequency microwave radiometer (SFMR) [*Uhlhorn et al.*, 2007] is another instrument for measuring surface winds. The SFMR measures brightness temperatures at six C-band channels, which increase in proportion to the area of sea surface foam coverage and absorption by rain drops, from which surface wind speed and path-integrated rain rate are ultimately retrieved. The SFMR provides an independent surface-wind measurement, not possible with Doppler radar, with greater accuracy than extrapolated flight-level winds and better horizontal coverage (i.e., 1 Hz output) than dropsondes. It can thus be of significant value to the forecasting and research communities [e.g., *Uhlhorn et al.*, 2007]. The purpose of this paper is to use flight-level and SFMR surface wind measurements to document the evolution of wind asymmetries over a three-day time period in Hurricane Rita.

2. Storm Summary and Data

[5] Hurricane Rita was the fourth major hurricane (Saffir-Simpson Category 3 or greater) of the 2005 Atlantic hurricane season. Rita tracked nearly due west in the Gulf of Mexico as a Category 5 hurricane on September 21 with observed peak surface winds of ~ 70 m s^{-1}. On September 22 Rita weakened slightly and turned toward the northwest, maintaining its forward speed. As it approached the Texas/Louisiana border, Rita weakened to a Category 3 hurricane, eventually making landfall on September 24. During this time period, Rita exhibited considerable asymmetries in both its wind and rain fields [*Houze et al.*, 2007].

[6] As Rita traversed the Gulf of Mexico between 21–23 September, NOAA and NRL P-3 aircraft sampled the storm. The data shown here are from one NOAA P-3 aircraft, which flew two "figure-4" patterns with radial legs in each storm quadrant for each flight from 21–23 September. These radial legs were oriented approximately along and

---

[1]Hurricane Research Division, AOML, NOAA, Miami, Florida, USA.

Along storm track

(a)

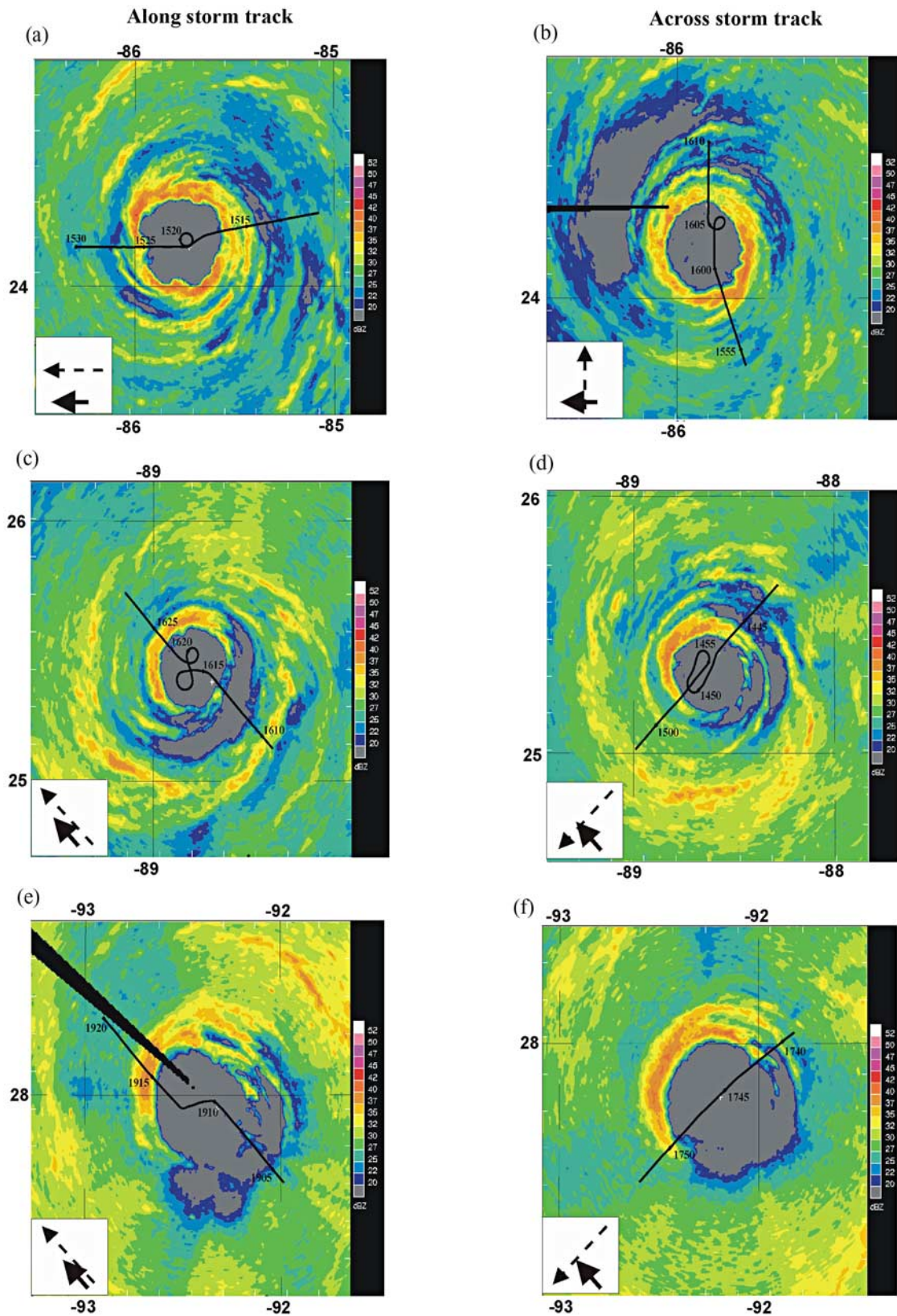**Across storm track**

(b)

(c)

(d)

(e)

(f)

Figure 1. NOAA P-3 lower fuselage radar images with flight tracks overlaid (shaded, dBZ, scale showed on right-hand side of figure) for (a) 1519 UTC 21 Sept., (b) 1606 UTC 21 Sept., (c) 1614 UTC 22 Sept., (d) 1447 UTC 22 Sept., (e) 1910 UTC 23 Sept., and (f) 1745 UTC 23 Sept. Inset indicates approximate direction of storm track (bold arrowhead) and orientation of flight leg relative to storm track (dashed arrow). Radar images are 160 km on a side. Left (right) plots show flight tracks along (across) storm track.
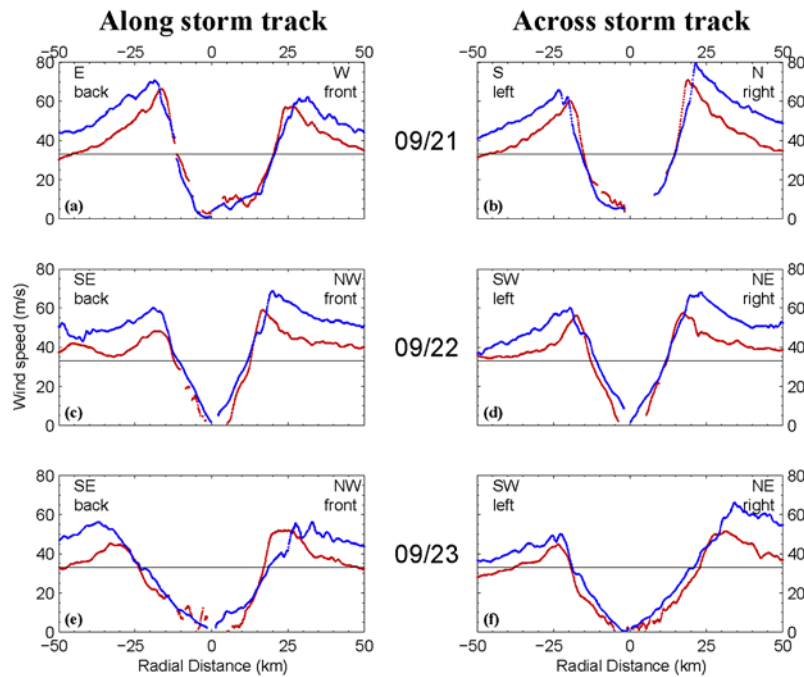
Figure 2. Time series (converted to distance from storm center in km) of earth-relative flight level wind speed (blue, m s^{-1}) and SFMR surface wind speed (red, m s^{-1}) for flight legs shown in Figure 1. (a) 1505–1534 UTC September 21, (b) 1550–1616 UTC September 21, (c) 1552–1647 UTC September 22, (d) 1427–1521 UTC September 22, (e) 1845–1937 UTC September 23, and (f) 1721–1812 UTC September 23. Left (right) plots present flight legs along (across) the storm track. "Left", "right", etc. designations refer to locations left, right, etc. from storm track. Horizontal line denotes threshold of hurricane-force winds.

across the storm track, at altitudes between 3.1 and 3.7 km. Flight-level and SFMR wind data were collected on each day.

3. Observations of the Evolution of Surface and Flight-Level Wind Field Asymmetries

[7] Figure 1 shows P-3 lower fuselage (LF) radar reflectivity images during each of the three days the aircraft was in the storm. On September 21 the eyewall is closed and the eye is ~ 40 km in diameter. On the next day, the LF pattern suggests that Rita has a concentric eyewall pattern (Figures 1c and 1d) confirmed by *Houze et al.* [2007]. The inner eyewall has contracted to ~ 30 km diameter and an outer eyewall 90 km in diameter is evident. By September 23 (Figures 1e and 1f) the inner eyewall from the previous day has dissipated and the outer eyewall has contracted to ~ 60 km diameter. Also during these three days, the reflectivity pattern evolves from being symmetric to demonstrating a wavenumber-1 asymmetry, with a maximum in the front side of the storm, relative to storm track.

[8] Radial profiles of earth-relative flight-level and SFMR surface winds for one figure-4 pattern each day are shown in Figure 2, with summary statistics contained in Table 1 (only one figure-4 pattern is shown from each day to highlight interday variability). On September 21, there are variations in the peak wind speed at flight-level and the surface both across and along the storm track, with maximum values in the right (north) and back (east) quadrants. The largest peak values are found in the right (north) quadrant, which would be expected for a translating sym-

metric hurricane [*Shapiro*, 1983]. On September 22, the along-track peak reverses to the front of the storm, but the across-track peak remains on the right side of the track. By September 23, there is very little variation in the peak winds in the along-track direction, but there is a significant variation in the across-track direction at both levels, with peak values on the NE side of the storm and a 16 m s^{-1} difference in across-track peak flight-level wind speed (cf. Table 1). The magnitude of the across-track asymmetry on

Table 1. Maximum Earth-Relative Wind Speed and Radius of Maximum Wind (RMW, km) at Flight Level and the Surface for Each of the Four Flight Legs on September 21–23[a]

	September 21	September 22	September 23
V_{max} (m s^{-1}) (flight-level/surface)			
front	62.2/57.2	68.7/59.0	56.3/52.0
right	79.8/71.0	68.0/57.5	66.2/51.6
rear	70.8/66.4	60.1/48.2	56.1/45.3
left	65.9/60.4	60.1/56.2	50.2/44.8
RMW (km) (flight-level/surface)			
front	31.3/26.0	20.0/16.7	32.9/23.9
right	21.6/18.9	23.4/17.6	34.3/31.6
rear	18.7/16.9	19.0/18.7	36.9/33.0
left	23.3/19.9	19.6/17.5	22.8/23.3
Storm motion			
heading (deg)	275	300	320
translational speed (m s^{-1})	5.5	4	5

[a]V_{max} is wind speed (m s^{-1}), and RMW is radius of maximum wind. Data are grouped according to location of flight leg relative to the storm track: front and rear (along storm track), and right and left (across storm track). Storm heading and forward translational speed are also provided.
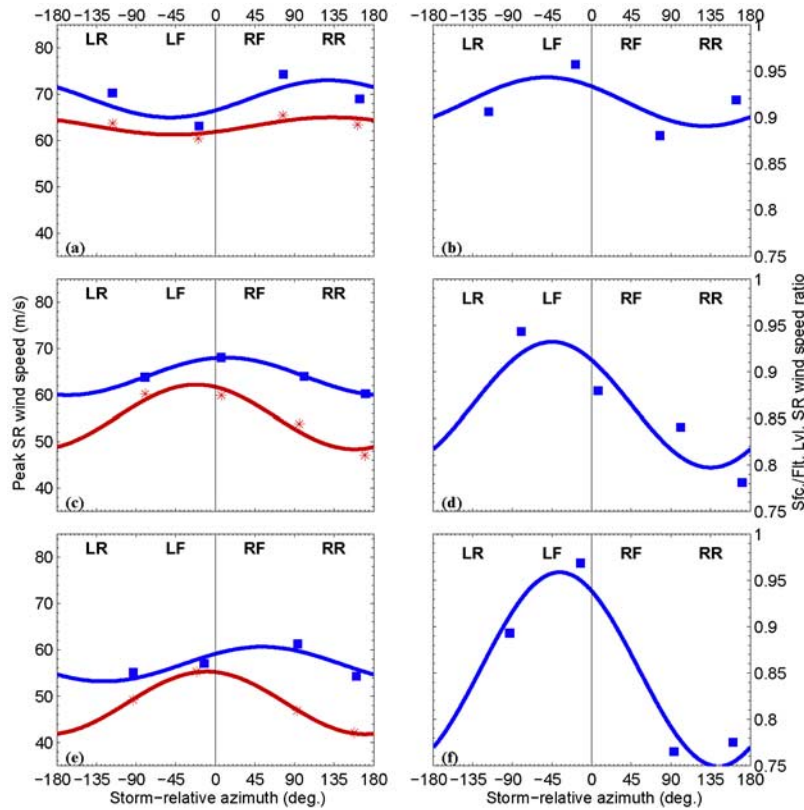
Figure 3. (left) Azimuthal variation of storm-relative peak flight-level (blue, m s^{-1}) and surface (red, m s^{-1}) winds on (a) September 21, (c) September 22, and (e) September 23. Azimuthal locations are plotted relative to storm track, with positive (negative) values denoting locations to the right (left) of storm track. (right) Azimuthal variation of r, ratio of peak surface to flight-level winds for (b) September 21, (d) September 22, and (f) September 23. Acronyms "LR", "LF", "RF", and "RR" denote left-rear, left-front, right-front, and right-rear quadrants, respectively.

this day is larger than twice the storm translational speed (5 m s^{-1}, cf. Table 1).

[9] A notable evolution in the relationship between the surface and flight-level winds across the entire leg also occurs over the three days. On September 21 the surface winds are less than flight-level by a nearly constant value of 10–15 m s^{-1} both along and across the storm track. On September 22, the surface winds, on average, are less than the flight-level winds by nearly the same amount on both sides of the along-track leg, but the difference between surface and flight-level winds is greater to the right of track than left of track. By September 23, the surface winds on the back side of the storm are less than the flight-level winds by a greater amount than on the front side. Also, a significant variation is evident in the across-track direction, with the surface winds less than flight-level winds by ~5 m s^{-1} (15–20 m s^{-1}) on the left (right) side of the storm track. From these comparisons it is clear that, while there are azimuthal asymmetries in the flight-level and surface winds on all three days, the magnitude and phase of the asymmetries vary from day to day. Furthermore, the change with height of the phase of the asymmetries between the surface and the flight-level, i.e., phase shift, changes over time.

[10] For comparison with previous studies [e.g., *Kepert*, 2001, 2006a, 2006b; *Kepert and Wang*, 2001], storm-relative winds are calculated based on storm motion from Table 1. Figure 3 shows the evolution of the peak storm-

relative wind asymmetry phase, with summary statistics in Table 2. For each radial leg, the peak flight-level and surface wind speed and azimuthal location (relative to storm motion) are plotted. A wavenumber-1 sinusoidal function is fit using least-squares to the data to identify the amplitude and phase of the asymmetric wind at both levels. On September 21, both the surface and the flight-level winds show a pronounced asymmetry, with the phase of the

Table 2. Azimuthal Fits to Storm-Relative Wind Speed, Ratio of Surface to Flight-Level Winds, and Eyewall Slope[a]

	September 21	September 22	September 23
Speed (v) (flight-level/surface)			
$\bar{v}$ (m s^{-1})	69/63.1	64/55.3	56.9/48.5
v' (m s^{-1})	4/1.9	4/6.9	3.7/6.7
Φ_v (deg)	128.6/132.6	12/−21.6	53.5/−9.9
Ratio of surface to flight-level winds (r)			
$\bar{r}$ (dimensionless)	0.92	0.86	0.85
r' (dimensionless)	0.03	0.07	0.1
Φ_r (deg)	−51.1	−44.9	−36.3
Eyewall slope (s)			
$\bar{s}$ (dimensionless)	0.90	0.94	1.28
S' (dimensionless)	0.36	0.81	1.36
Φ_S (deg)	−40.3	53.4	26.2

[a]Here v is azimuthal fits to storm-relative wind speed, r is ratio of surface to flight-level winds, and s is eyewall slope (tan θ from Figure 4a). Values plotted are azimuthal mean (overbar), amplitude of variation (prime), and azimuthal phase (Φ, relative to storm track).
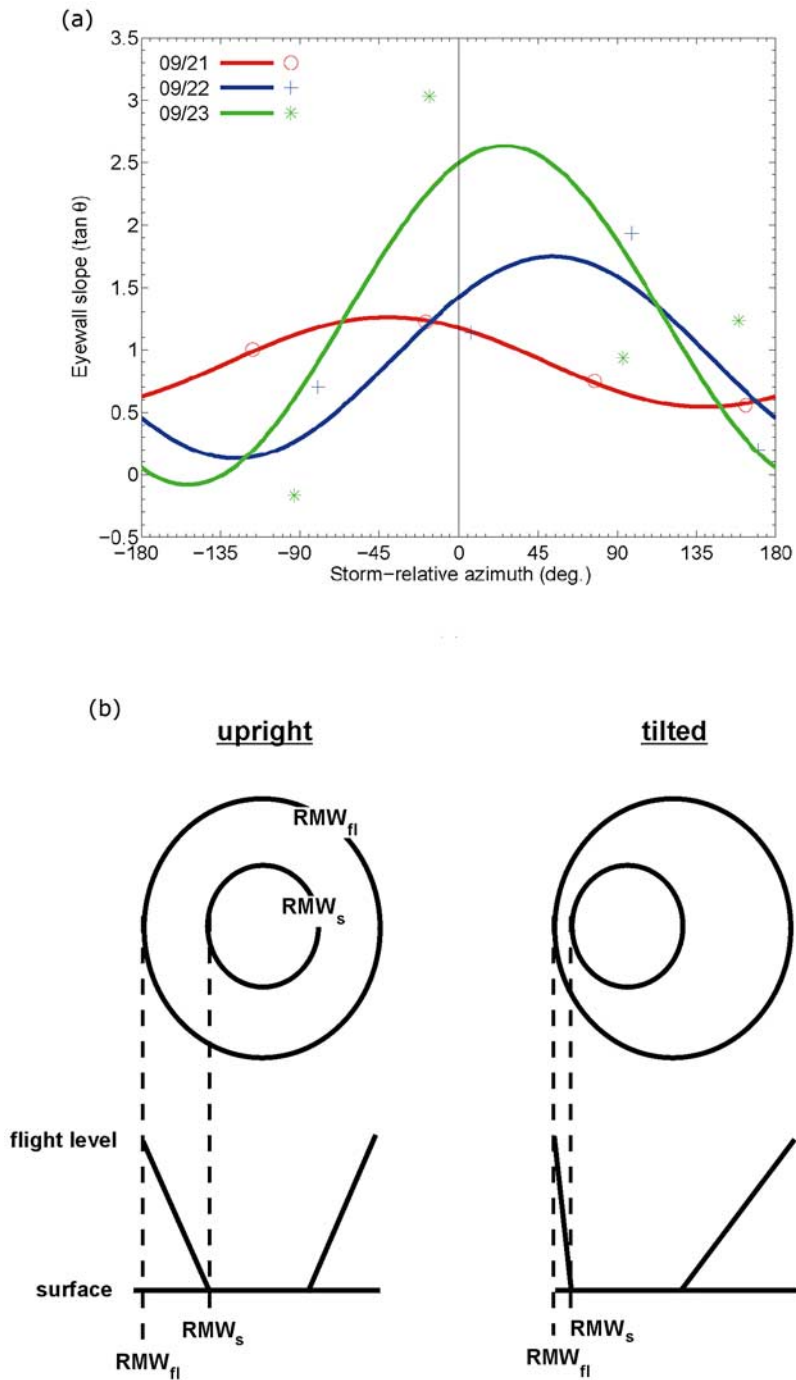
Figure 4. (a) Azimuthal variation of radius of maximum wind slope (s = tan θ, dimensionless) for September 21 (red), September 22 (blue), and September 23 (green). Azimuthal locations are plotted using same convention as Figure 3. (b) Idealized schematic showing plan view (top row) and vertical cross sectional (bottom row) differences in RMW at the surface (RMW$_s$) and at flight-level (RMW$_{fl}$) for vertically-upright vortex and tilted vortex. Eyewall slope denoted by tan θ, where θ represents the angle of the RMW with respect to the vertical.

asymmetry at both levels about 130 degrees to the right of storm track, i.e., the right-rear quadrant relative to storm track. Because the phase at each level is nearly the same, the ratio of peak surface to peak flight-level winds around the storm (*r* in Table 2) varies comparatively little, ranging between 0.89 and 0.95. On the next day the phase of the surface and flight-level winds both shifts to the front side of the storm, with about a 30-degree phase shift upwind with

height consistent with previous theoretical and observational studies [*Kepert*, 2001, 2006a, 2006b]. By the third day, there is a considerable phase shift of ∼60 degrees in the peak winds between the two levels. Consequently, the peak wind ratio on September 23 varies between 0.75 and 0.95, a much larger azimuthal variation than on September 21. The phase of the asymmetry in the peak wind ratio, found on the left side of the storm track on all three days, is also

consistent with boundary layer numerical modeling and observational studies of tropical cyclones [*Kepert*, 2001, 2006a, 2006b; *Kepert and Wang*, 2001].

[11] Other information about the wind field structure at the surface and flight-level can be determined by examining the radii of maximum wind (RMW) at both levels around the storm. Since the RMW in mature tropical cyclones normally slopes outward with height [*Marks and Houze*, 1987], the RMW at the surface is usually smaller than at flight-level. An azimuthal variation in the RMW slope indicates a vortex that is tilted in the vertical. Figure 4a shows RMW slope (s) between the surface and flight-level around the storm, defined as radial displacement/altitude (equal to tan θ, where θ is measured relative to vertical, Figure 4b). Slope values are plotted from each of the four radial legs on each day, and a wavenumber-1 function is fit to the data. The variation in the slope of the RMW around the storm steadily increases over the three days, reaching a maximum on September 23. This increase over time in the azimuthal variation of the slope suggests that the vortex tilt is increasing over time, though more data at intermediate levels is needed to confirm this hypothesis. This increase in tilt is associated with enhanced azimuthal variations in the ratio of surface to flight-level winds (see Figure 4b for a schematic illustrating this). The phase of the slope, i.e., the direction the vortex tilts, also changes over time, from 45 degrees to the left of storm track on September 21 to 30 degrees to the right of storm track on September 23.

4. Summary and Future Work

[12] Hurricane Rita experienced significant evolution in its surface and flight-level wind fields during the three days it traversed the Gulf of Mexico. The wind fields showed an asymmetry on all three days, but the characteristics of the asymmetry, in particular the relationship between the surface and flight-level winds, varied over time. On September 21 the azimuthal asymmetries in the wind fields were aligned in the vertical, with peak values to the right side of storm track, in agreement with previous modeling and observational studies [*Shapiro*, 1983]. Over the next two days the phases diverged, so that by September 23 there was a 60-degree rotation in the phase of the asymmetry between the surface and flight level. The ratio of surface to flight-level wind maxima was peaked on the left side of the storm track on all three days, consistent with *Kepert* [2001, 2006a, 2006b] and *Kepert and Wang* [2001]. However, the amplitude of the asymmetry increased markedly during the three days. Concurrent with the increase over time in the phase shift of the asymmetry was an increase in the azimuthal variations in RMW slope, indicative of increasing vortex tilt.

[13] The magnitude of the across-track wind variation, and the phase shift in peak winds between the surface and flight-level, can not be explained solely by storm motion.

Vertical shear of the horizontal wind may explain the structures in both the wind field and the reflectivity field. Preliminary analyses of the inner-core vertical shear from airborne Doppler radar (not shown) indicate that shear was increasing during the three days. Further analysis of this mechanism is left for future work.

[14] Since the data used in this study were derived from aircraft flying figure-4 patterns with four azimuths sampled, only the wavenumber-0 and -1 components were resolved. It is possible that higher wavenumber features have been aliased onto the wavenumber-1 fields. Future work will involve incorporating additional data sets, notably airborne Doppler radar, dropsonde measurements, and high-resolution numerical model simulations, into the analysis of the wind field evolution of Rita. These additional data sets will allow for the ability to resolve higher wavenumber features, providing a more complete three-dimensional picture of the storm and allowing an identification of the processes responsible for the structure and evolution of the asymmetries shown here.

References

Franklin, J. L., M. L. Black, and K. Valde (2003), GPS dropwindsonde wind profiles in hurricanes and their operational implications, *Weather Forecast.*, *18*, 32–44.
Houze, R. A., Jr., S. S. Chen, B. F. Smull, W.-C. Lee, and M. M. Bell (2007), Hurricane intensity and eyewall replacement, *Science*, *315*, 1235–1239.
Kepert, J. D. (2001), The dynamics of boundary layer jets within the tropical cyclone core. Part I: Linear theory, *J. Atmos. Sci.*, *58*, 2469–2484.
Kepert, J. D. (2006a), Observed boundary layer wind structure and balance in the hurricane core. Part I: Hurricane Georges, *J. Atmos. Sci.*, *63*, 2169–2193.
Kepert, J. D. (2006b), Observed boundary layer wind structure and balance in the hurricane core. Part II: Hurricane Mitch, *J. Atmos. Sci.*, *63*, 2194–2211.
Kepert, J. D., and Y. Wang (2001), The dynamics of boundary layer jets within the tropical cyclone core. Part II: Nonlinear enhancement, *J. Atmos. Sci.*, *58*, 2485–2501.
Marks, F. D., Jr., and R. A. Houze Jr. (1987), Inner core structure of Hurricane Alicia from airborne Doppler radar observations, *J. Atmos. Sci.*, *44*, 1296–1317.
Powell, M. D. (1987), Changes in the low-level kinematic and thermodynamic structure of Hurricane Alicia (1983) at landfall, *Mon. Weather Rev.*, *115*, 75–99.
Reasor, P. D., M. T. Montgomery, F. D. Marks Jr., and J. F. Gamache (2000), Low-wavenumber structure and evolution of the hurricane inner core observed by airborne dual-Doppler radar, *Mon. Weather Rev.*, *128*, 1653–1680.
Schneider, R., and G. M. Barnes (2005), Low-level kinematic, thermodynamic, and reflectivity fields associated with Hurricane Bonnie (1998) at landfall, *Mon. Weather Rev.*, *133*, 3243–3259.
Shapiro, L. J. (1983), The asymmetric boundary layer flow under a translating hurricane, *J. Atmos. Sci.*, *40*, 1984–1998.
Uhlhorn, E. W., P. G. Black, J. L. Franklin, M. Goodberlet, J. Carswell, and A. S. Goldstein (2007), Hurricane surface wind measurements from an operational stepped frequency microwave radiometer, *Mon. Weather Rev.*, *135*, 3070–3085.

———————————
R. Rogers and E. Uhlhorn, Hurricane Research Division, AOML, NOAA, 4301 Rickenbacker Causeway, Miami, FL 33149, USA. (Robert.Rogers@noaa.gov)